Gamma-Compression Gamut Mapping Method Based on the Concept of Image-to-Device

Hung-Shing Chen,▲* Minoru Omamiuda and Hiroaki Kotera▲

Graduate School of Science and Technology, Chiba University, Inage-ku, Chiba, Japan

** Communication & Information Technology Laboratory, Dai Nippon Printing Co., Ltd., Shinjuku-ku, Tokyo, Japan*

This article proposes Gamma-Compression Gamut Mapping Algorithm (GMA) based on the concept of Image-to-Device. Considering the relations of color gamut boundaries between the devices (such as printer, monitor) and image source, the proposed method adjusts the image color distributions, fitting to the output device gamut. The proposed image-to-device GMA works to preserve its gradation and chroma with minimum losses depending on the color distributions in the segmented hue-leaves. The following three typical mapping methods are compared and discussed: (1) *Device-to-Device Gamma-Compression* GMA, (2) *Image-to-Device Gamma-Compression* GMA; (3) *Clipping* GMA. Two kinds of color spaces, CIEL*a*b* and CIECAM97s-JCh, are used for testing these GMAs. The psychophysical experiments in CIECAM97s-JCh space resulted in better rendition than did CIEL*a*b* space. In natural color imaging applications, the proposed *Image-to-Device* GMA is superior to conventional *Device-to-Device* GMA, and is a better way to maintain its gradation and higher chroma.

Journal of Imaging Science and Technology 45: 141–151 (2001)

Introduction

In the process of digital color reproduction, a key feature is the use of gamut mapping techniques to adjust the different color gamuts between displays and printers. However, most of the current gamut mapping techniques are based on the concept of Device-to-Device (D-D), which neglects the image color distributions.

Even though the concept of Device Independent Color has gradually been applied to many color management systems in image input and output devices, it is not enough to solve the color appearance problems among different devices, particularly between the monitor and printer. In the same surrounding viewing conditions of color temperature and luminance, color appearance mismatch between these two devices comes from the difference in their color gamut sizes. Usually the monitor's gamut is wider than the printer's gamut. To resolve this problem, establishment of a gamut mapping algorithm (GMA), based on the concept of Image-to-Device (I-D), becomes important.

Recently, an image-dependent remapping strategy was developed by Braun and Fairchild.[1] This nonlinear GMA coupled with sigmoidal lightness rescaling functions and chroma remapping functions performs better than the typical D-D linear GMAs for pictorial images. When the nonlinear GMA is utilized, it is possible to enhance the perception of lightness and chroma, although the dynamic ranges of image were scaled down after mapping.

Original manuscript received June 19, 2000

▲ IS&T Member

In this article, (1) the nonlinear Gamma-Compression GMA based on I-D concept, which is coupled with a gamma-compression coefficient γ and hue-leaf division is discussed and (2) experiments on appearance comparison between CIEL*a*b* and CIECAM97s-JCh[2] (the simple version of CIE Color Appearance Model) spaces are reported.

The Basic Idea of Gamut Mapping

Gamut mapping means that projection from the color points within image source's gamut ***i*** (input) to the points within destination device's gamut ***o*** (output). If the gamut ***i*** is located inside the gamut ***o, i*** remains as it is. If the gamut ***i*** lies over or across the gamut ***o***, the compression for ***i*** will be necessary. When the gamut mapping is executed, the gamut relationship between the source image and the destination device should be considered. Printing the images on the monitor is a typical application for gamut mapping. Because CRT gamut is usually wider than printer gamut in most color spaces, gamut compression from the CRT gamut into the printer gamut has been performed in many cases. In the mapping process, the relations in three different gamuts of source image, CRT and printer must be taken into account. In general, the device gamuts are defined by the measured color values or mathematical models, but the image gamut cannot be modeled due to its random distributions of color. Thus the GMA can be designed based on the following two relations:

(1) **Device-to-Device** (From CRT gamut to printer gamut, called D-D)
(2) **Image-to-Device** (From image gamut to printer gamut, called I-D)

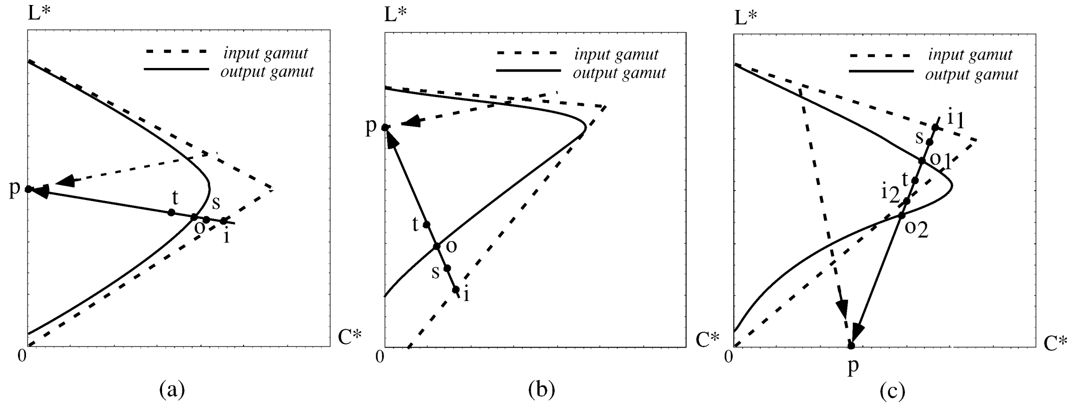

Figure 1. Overview of the relationship between input gamut and output gamut.

In case (1), if the color gamut of source image is regarded as the same as the CRT gamut, the GMA based on D-D concept is easy to design. Most current compression methods are based on this concept. However, if CRT gamut is not congruent with the source image, losses in gradation and chroma due to over-compression will happen. In case (2), the color information losses after mapping will be kept to a minimum by compressing the image colors from outside the gamut boundary into the printer gamut. The Clipping method is the simplest GMA to keep the color distributions unchanged inside the printer gamut, while all the colors outside the printer gamut are compressed into the gamut boundary losing their gradations.

The following three important factors should be taken into account to design the GMA.

(1) the extraction of gamut boundaries.
(2) the decision of compression direction and the calculation of intersections on gamut boundaries.
(3) the decision of gamut compression function.

In the proposed GMA, first, the two-dimensional gamut boundaries are extracted from the measured color chips of printer and the color distributions of image in the hue-divided lightness-chroma planes. Secondly, the I-D gamma-compression with coefficient γ, is performed in each hue-leaf.

Gamut Mapping Algorithms

Gamut Compression in Lightness-Chroma Plane

The cross sections of color gamut boundaries for printer and image are illustrated in L*-C* plane of CIEL*a*b* space as shown in Fig. 1. The gamut relations between the input data and the output device are classified into three different cases. In cases (a) and (b), the input gamut is completely enclosed by the output gamut, where Eq. 1 is used to compress the source colors along a given line toward $\boldsymbol{p}$ on the L* axis. In case (c), the input gamut is not fully enclosed by the output gamut, but they cross over each other, where Eq. 2 is used to compress the source colors along a given line toward $\boldsymbol{p}$ on the C* axis.

Several articles[3–4] discuss the decision rules for the focal points. Here, the focal point p is decided by reference to CARISMA[5] maps. The focal point $\boldsymbol{p}$ in case (a) represents the point of intersection between the line passing through the two gamut cusps and L* axis, and $\boldsymbol{p}$ in case (b) is the point of intersection between the L* axis and a line drawn parallel to C* axis that passes through the input gamut cusp. The point $\boldsymbol{p}$ in case (c) lies on C* axis whose chromatic value is half of the maximum chroma of the output gamut.

The proposed Gamma-Compression GMA,[5] which is advanced from CARISMA[4] maps, is performed based on the following set of equations in Lightness-Chroma plane of CIEL*a*b* or CIECAM97s-JCh.

$$\overrightarrow{pt} = \overrightarrow{po} \cdot \left(\frac{\overline{ps}}{\overline{pi}} \right)^{\gamma} \text{; for cases (a) and (b) in Fig. 1} \quad (1)$$

$$\overrightarrow{pt} = \overrightarrow{po_2} + \overrightarrow{o_2 o_1} \cdot \left(\frac{\overline{i_2 s}}{\overline{i_2 i_1}} \right)^{\gamma} \text{; for case (c) in Fig. 1} \quad (2)$$

Here, $\boldsymbol{s}$, $\boldsymbol{t}$, $\boldsymbol{o}$ ($\boldsymbol{o}_1$, $\boldsymbol{o}_2$), $\boldsymbol{i}$ ($\boldsymbol{i}_1$, $\boldsymbol{i}_2$) and $\boldsymbol{p}$ represent the positions of input color, target color, the output gamut, the input gamut and the focal point in Lightness-Chroma plane respectively. The gamma-compression coefficient γ must be set between 0 and 1, but the actual range is determined by the experiments. The GMA works as linear compression for $\gamma = 1$, and as nonlinear compression for $0 < \gamma < 1$.

Color Spaces

It is desirable that gamut mapping be performed in a uniform color space. The current GMAs almost use CIEL*a*b* space, because it has better uniformity and is easy to calculate. However, it is reported that the bluish loci at equal hue angle are not on straight lines in CIEL*a*b* space, but on curved lines. While, the JCh color space of CIECAM97s[6] (the simple version of CIE Color Appearance Model) was reported to have the better blue hue loci than CIEL*a*b* space.[3] The color conversion to CIECAM97s space is shown in Fig. 2. The chromatic adaptation in CIECAM97s includes the linear Bradford transformation with M_{BFD} matrix and the nonlinear transformation using surround data and parameters, i.e., the luminance of adaptation field, the tristimulus value of light source, the relative luminance of background, the lightness contrast factor, the degree of adaptation, and so on. Then the data of color appearance correlates in CIECAM97s; lightness J, chroma C and hue angle h are obtained.

To estimate the appearance fitness to color spaces , the proposed GMA and other methods are tested in both CIE L*a*b* and CIECAM97s.

In this study, the Lightness-Chroma (L-C) plane of CIE L*a*b* space is represented as its chroma value: C

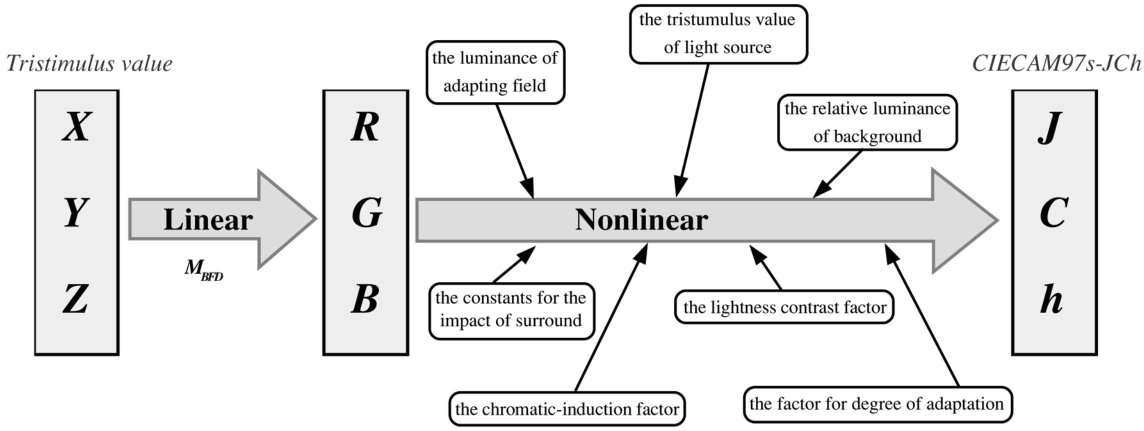

Figure 2. Color transformation to CIECAM97s–JCh space.

= $(a^{*2} + b^{*2})^{0.5}$ and lightness value: L*, while the L-C plane in CIECAM97s-Jch is defined as its chroma value C and lightness value J. Furthermore, C . sinh-C . cosh plane in CIECAM97s space is defined corresponding to the a*–b* plane in CIE L*a*b* space.

Hue-Leaf Division

To decide the gamut boundary functions in the L-C planes of CIE L*a*b* and CIECAM97s-Jch, the hue-leaf divisions for the color data of input sources, i.e., monitor and image, and output sources, i.e., printer, are necessary. In the experiment, the L-C planes are segmented into 6 main hue-leaves of red, yellow, green, cyan, blue, and magenta (r, y, g, c, b, m) in CIE L*a*b* and CIECAM97s-JCh space as shown in Table I.

Based on the color name categories, each hue angle range in testing color spaces is divided unevenly according to the subjective observations for the actual test images as shown in Table I.

Because the hue uniformities are different between CIE L*a*b* and CIECAM97s-JCh spaces, each angle range of hue division must be found individually. According to the angle ranges after division, the color distributions of image or monitor are segmented into 6 main hue-leaves in a* – b* plane of CIE L*a*b* and $C \bullet \sin(h) - C \bullet \cos(h)$ plane of CIECAM97s-JCh.

The monitor gamut boundary functions can be calculated from model-based color transformation. However, the printer models are difficult to characterize physically; thus its gamut boundary functions have been obtained from the measured values of printed color charts.

Initial data sets of {x, y, z} for testing color spaces, i.e., the data {a*b*L*} in CIE L*a*b* and the data {$C \bullet sinh$, $C \bullet cosh$, J} in CIECAM97s-JCh, are generated with equal intervals of $\Delta x = 10$, $\Delta y = 10$, $\Delta z = 5$ in the ranges of $-120 \le x \le 120$, $-120 \le y \le 120$, $0 \le z \le 100$ respectively. The corresponding initial RGB data have been limited within the sRGB range and located between 0 and 1. Thus 1675 sets of {a*,b*,L*} values and 2823 sets of {$C \bullet \sin(h)$, $C \bullet \cos(h)$, J} values on sRGB monitor are obtained (see Figs. 3a and 3c).

The high quality color chips from these L*a*b* and JCh data on the sRGB monitor (Sony/GDM-2000 TC) are printed on superfine paper (Epson/Photographic superfine paper) with high quality halftone by Epson PM-750C inkjet printer respectively. XYZ tristimulus values of the printed chips are measured with Gretag spectrophotometer and then transformed into CIE L*a*b* and CIECAM97s-JCh values (see Figs. 3b and 3d). Here, the hue-division LUTs are used to segment the measured chip data corresponding to the main hue-leaves in Table I.

TABLE I. Segmented Hue-Leaves.

(a) 6 hue-leaves segmented in CIEL*a*b* space.

Hue-leaf	Angle range (CIEL*a*b*)
red	0 ~ 80 & 355 ~ 360 degrees
yellow	80 ~ 115 degrees
green	115 ~ 185 degrees
cyan	185 ~ 245 degrees
blue	245 ~ 320 degrees
magenta	320 ~ 355 degrees

(b) 6 hue-leaves segmented in CIECAM97s space.

Hue-leaf	Angle range (CIECAM97s)
red	0 ~ 70 & 350 ~ 360 degrees
yellow	70 ~ 115 degrees
green	115 ~ 210 degrees
cyan	210 ~ 235 degrees
blue	235 ~ 305 degrees
magenta	305 ~ 350 degrees

According to six main hue-leaves of r,y,g,c,b,m in Table I, the extracted color points of image, monitor, and printer are projected onto L-C plane in CIE L*a*b* and CIECAM97s-JCh spaces, and the color distributions on the L-C plane (L-C distributions) are obtained. Next, each gamut boundary function is mathematically described by fitting to the cross section shapes of the segmented L-C distributions.

Gamut Boundary Functions

The gamut boundary function is calculated by extracting the most outside color points from L-C distributions at the segmented main hue-leaves. It is classified into two categories below.

Device Gamut Boundary Function (CRT or Printer)

For the device's C-L distributions (CIE L*a*b* and CIECAM97s-JCh), L axis is divided into 25 pieces by equal intervals between minimum and maximum of

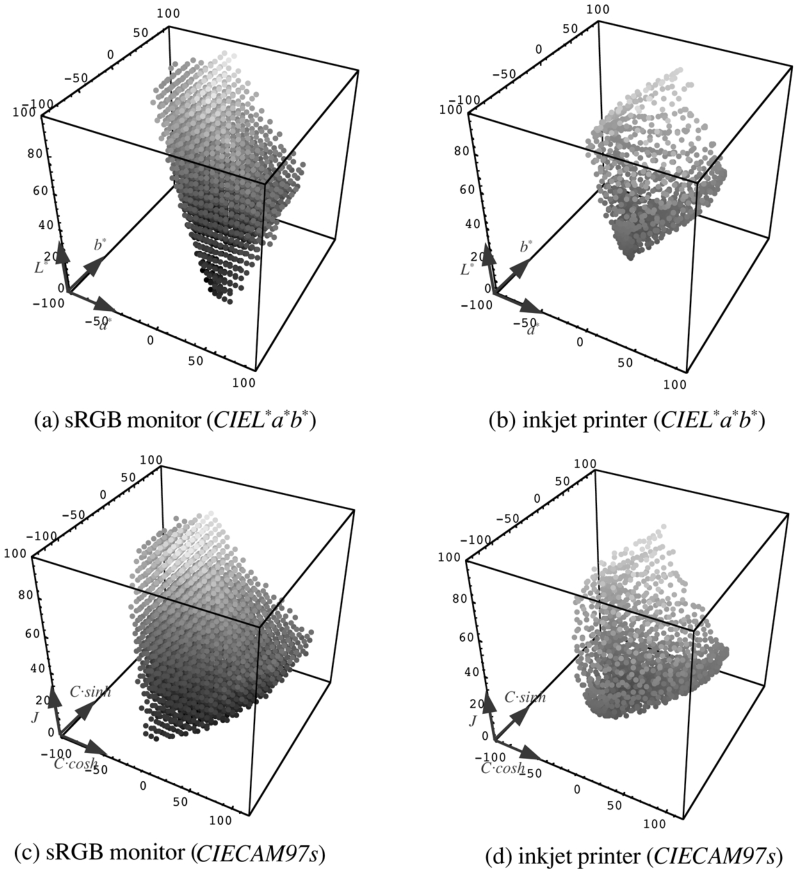

Figure 3. Color distributions of sRGB monitor and inkjet printer in CIEL*a*b* and CIECAM97s spaces.

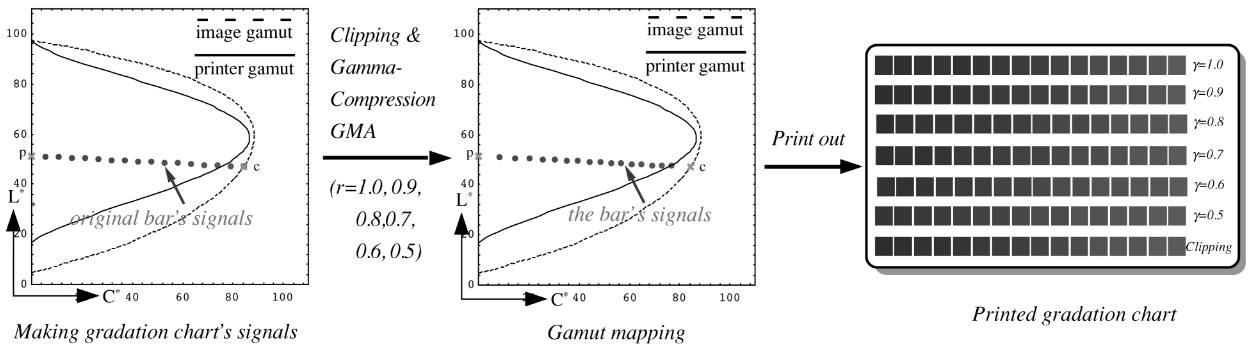

Figure 4. Process of making gradation charts for estimating the fitting γ value.

their L values. The least-squares method is applied to fit the data of these maximum chroma points located in each divided L interval; then the device gamut boundary function is obtained as a polynomial expansion.

Image Gamut Boundary Function

Seeking the image gamut boundary function is similar to that of the device. For the image C-L distributions, L axis is divided into 25 equal intervals between minimum and maximum L values. The image gamut boundary function can also be obtained by the method of the least-squares curve fitting to these maximum chroma points. However , the image data points are not distributed uniformly. If the divided L intervals don't include any data point, an approximatly smooth curve is obtained by interpolation from near by points.

Gamut boundary function is calculated by the following least-squares method.

The gamut boundary function $\boldsymbol{C_{bound}}$ is approximated by the m-th order polynomial expansions of variable L.

$$\boldsymbol{C_{bound}} = f(L) = a_1L + a_2L_2 \dots + a_mL^{m-1} \tag{3}$$

The coefficients $\{a_j\}$; j = 1~m are selected to minimize the mean square errors for n sets of maximum chroma points $\{C_i, L_i\}$; i = 1~n in each subdivided L interval

$$\varepsilon^2 = \sum_{i=1}^{n} \left[f(L_i) - C_i \right]^2 \tag{4}$$

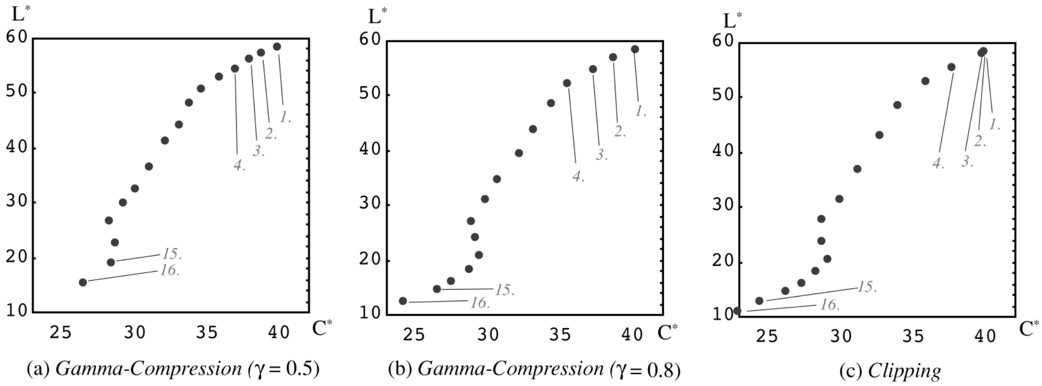

Figure 5. Color distribution on L*–C* plane of blue gradation chart mapped by Gamma-Compression with γ = 0.5 and 0.8 and Clipping Method.

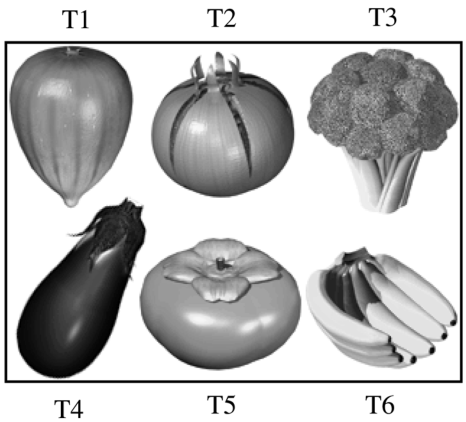

Figure 6. Test CG image: "fruits & vegetables".

$$\frac{\partial}{\partial a_j}\varepsilon^2 = 0,_{j=1\sim m} \quad (5)$$

Here, m = 4~5 th order polynomials are used for the curve fitting.

Gamma-Compression Coefficient

Because the gradation reproducibility strongly depends on γ values of Gamma-Compression GMA, the gamma-compression coefficient g must be predetermined before gamut mapping is applied. Here, the γ value has been determined by the experiments as follows. The process of making gradation charts is shown in Fig. 4. After completing the hue-leaf divisions of printer and image, 16 gradation steps with equal interval are selected along a given line segment **pc**, where **p** is the focal point on the L axis, and **c** is the maximum chroma point of segmented image. This maximum chroma point **c** is usually located on the gamut boundary of segmented image. Then those 16 gradation steps are converted into sRGB values and mapped by Clipping GMA and by Gamma-Compression GMA with γ = 1.0, 0.9, 0.8, 0.7, 0.6 and 0.5. Thus 7 different gradation bar charts are printed and their XYZ tristimulus values are measured with spectrophotometer (Gretag/Spectrolino).

Here, the measured gradation curves of blue color-hue on L-C plane in CIEL*a*b* space are shown in Fig. 5 and are analyzed as follows.

Clipping GMA loses the gradations out-of-gamut, especialy in the high lightness-chroma ranges, i.e., the overlapped points 1, 2, and 3 of Fig. 5(c), but preserves the correct L-C gradations inside of the printer gamut, i.e., points 4,...,16 of Fig. 5(c). This inside region reflects the widest chroma ranges and output L-C gradation charcteristics of the printing media. Comparing the shapes of L-C gradation curves between Clipping GMA and Gamma-Compress GMA by changing the γ values, these gradation steps preserved by Clipping GMA will provide a criterion to find the appropriate γ values so that gradation curve by the Gamma-Compression GMA approaches to that of Clipping.

The crooked portion in the lower chroma range comes from the characteristics of the inkjet printer. Analyzing the curves in Fig. 5, the L-C distributions of blue color-hue by Gamma-Compression for γ = 0.8 GMA seem to be near those of Clipping method except in the high lightness-chroma range.

Considering the measured gradation steps for the other 5 hues (r,y,g,c,m), the optimum γ values for all 6 hues lie in the range of 0.7 ~ 0.9 in CIEL*a*b*, and 0.6 ~ 0.8 in CIECAM97s-JCh.

Test Image

The test images appropriate to the gamut mapping have been chosen to satisfy the following two conditions:

(1) Color distributions of test image are wider than the printer gamut.

(2) Color hues in test image are as uniform as possible.

The test CG image "fruits & vegetables" shown in Fig. 6 is used in this experiment. Its color distributions plotted on a* – b* plane and $C \bullet \sin(h)$-$C \bullet \cos(h)$ plane are shown in Fig. 7. It has wide ranges of green, yellow and red colors. This test image has been synthesized from six independent CG images, *T1, T2,..., T6*. Each includes the quality estimation feature for GMA as listed in Table II. Notice that some components are suitable for the gradation test and others for the bluish hue loci or false contour tests. In Fig. 6, T1 and T2, the figs and pomegranates having yellow and red colors are designed for evaluating the image gradation; T3 broccoli and T6 banana have brilliant green and yellow colors for testing the saturation. T4 eggplant is composed of blue and magenta colors and used to judge bluish hue change after mapping. T5 persimmon contains highlights in yellow to red colors and is used to judge the false contours after mapping.

Viewing Method and Data Analysis

Viewing configuration in phychophysical experiment is illustrated in Fig. 8. For evaluating each subimage, a

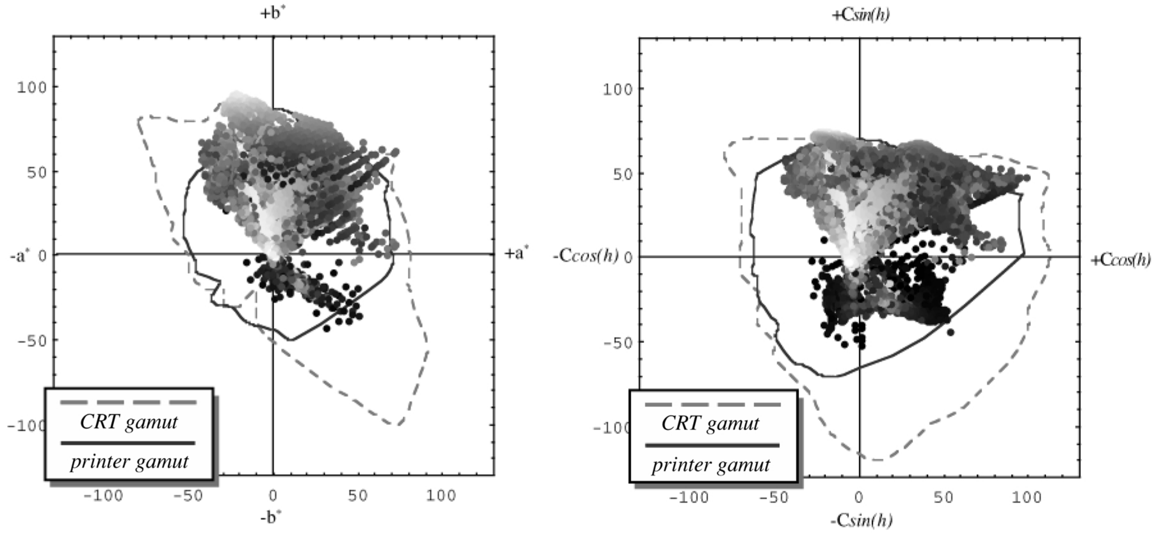

(a) a*-b*plane of CIEL*a*b* space (b) Ccos(h)-Csin(h) plane of CIECAM97s space

Figure 7. Gamut ranges of test iamge and devices plotted in two testing color spaces.

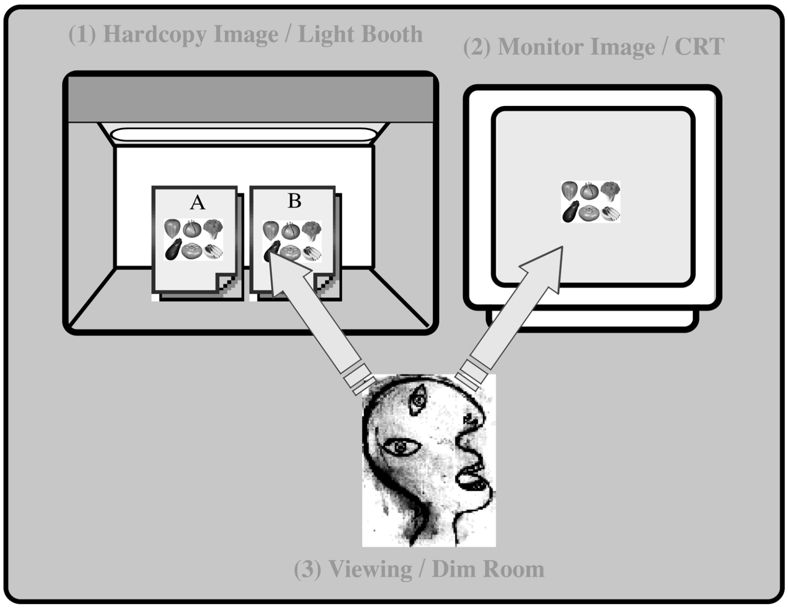

Figure 8. Viewing configuration in phychophysical experiment for gamut mapping.

TABLE II. Attention Points of 6 Subimages.

No.	Name	Color (hue)	Attention point
T1	fig	yellow + red	gradation
T2	pomegranate	yellow + red	gradation
T3	broccoli	green	all
T4	eggplant	blue + magenta	blue hue loci
T5	persimmon	yellow + red	false contour
T6	banana	yellow	all

psychophysical experiment was carried out to make a comparison of color appearance matching between the original CRT image (right side) and the printed hardcopies after mapping (left side). Both images were evaluated by 12 observers in dim viewing surroundings (approximately 64 lux). All observers are of normal color vision and have color experience in the field related to image processing, although they are not trained for the viewing technique. When $\boldsymbol{n}$ chosen GMAs are applied, $\boldsymbol{n}(\boldsymbol{n}-\mathbf{1})/\mathbf{2}$ pairs of hardcopy images are compared in an experiment according to the paired-comparison technique. The simulataneous binocular viewing technique is used in the paired-comparison experiment.[7] Note that each pair of hardcopy images is shown in a different and random order in the light booth, and the observers don't know what kinds of GMAs are used in hardcopy. The observers are asked to make a judgement on each subimage, which reproduction (A or B of pairs) in the light booth was closer to the original image on CRT monitor in terms of each subimage's attention point as shown in Table II.

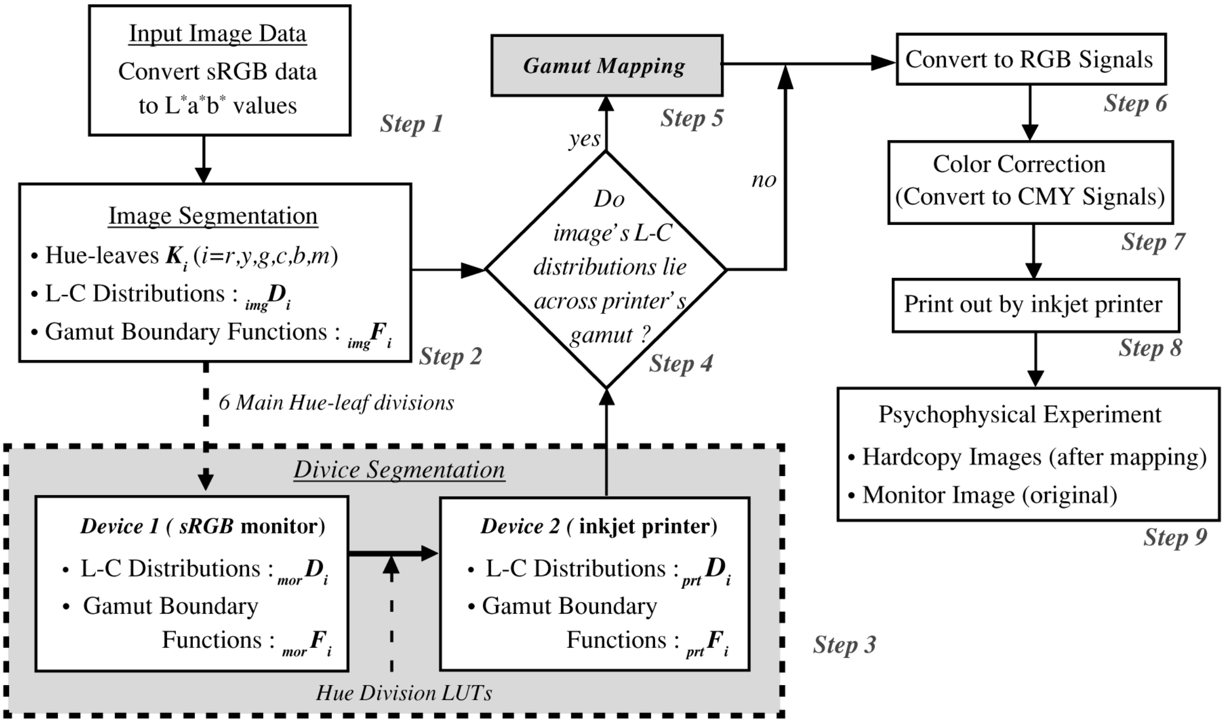

Figure 9. Flow diagram of gamut mappiong process.

TABLE III. An Example of z-Score Calculation: (a) Accumulated Matrix; (b) Frequency Matrix; (c) z-Score Matrix; and (d) z-Score Value.

(a) $a(i,j)$	Image 1	Image 2	Image 3	Image 4
Image 1	—	4	2	5
Image 2	8	—	9	5
Image 3	10	3	—	7
Image 4	7	7	5	—
(b) $f(i,j)$	Image 1	Image 2	Image 3	Image 4
Image 1	—	4	2	5
Image 2	8	—	9	5
Image 3	10	3	—	7
Image 4	7	7	5	—
(c) $z(i,j)$	Image 1	Image 2	Image 3	Image 4
Image 1	—	–0.4	–1.0	–0.2
Image 2	0.4	—	0.7	–0.2
Image 3	1.0	–0.7	—	0.2
Image 4	0.2	0.2	–0.2	—
(d) $z(i)$	Image 1	Image 2	Image 3	Image 4
z-score value	1.6	–0.9	–0.5	–0.2
Rank order	1	4	3	2

For obtaining the rank orders of tested GMAS, $\boldsymbol{n}(\boldsymbol{n}-\mathbf{1})/\mathbf{2}$ number of pair comparison data are analyzed by z-score values which are based on Thurstone's law of comparative judgement.[8]

An example of data analysis is listed in Table III. Assuming that 4 chosen GMAs, i.e., $\boldsymbol{n} = \mathbf{4}$, is applied to single subimages and 4 output hardcopy images (Image 1, Image 2, Image 3, and Image 4) are evaluated by 12 observer, then z-score values are calculated[9] as follows.

1. The accumulated number of times u is entered in the element $a(i,j)$ of accumulated matrix [see Table III(a)] during the experiment, which indicates *ith*-model is judged better *jth*-model $\boldsymbol{u}$ times. For example, if Image 1 and Image 2 are compared, the results of elements a(1,2) = 4 and a(2,1) = 8 in Table III(a) indicate that Image 1 is judged better 8 times and Image 2 is judged better 4 times during 12 times of total observations.

2. The element $a(i,j)$ of an accumulatedmatrix is converted to the frequency matrix according to Eq. 6 [see Table III(b)].

$$f(i,j) = \frac{a(i,j)}{a(i,j) + a(j,i)} \tag{6}$$

where $f(i,j)$ represents the element of frequency matrix.

3. The element $f(i,j)$ of frequency matrix are converted to the element $z(i,j)$ of z-score matrix according to Eq. 7 [see Table III(c)], where

$$f(i,j) = \frac{1}{\sqrt{2}} \exp\left(-\frac{\left(z(i,j)\right)^2}{2}\right). \tag{7}$$

4. The z-score value z(j) are calculated as a total of each column of z-score matrix, where

$$z(j) = \sum_i z(i,j)$$

[see Table III(d)].

Experiments

As shown in Fig. 9, the gamut mapping experiments have been carried out by the following procedures:

TABLE IV. Overview of test GMAs.

Mapping \ Compression	Linear	Nonlinear	Clipping
D–D	All color points shift linearly (γ = 1.0)	All color points shift nonlinearly (γ = 0.5 & 0.8)	—
I–D	All color points shift linearly (γ = 1.0)	All color points shift nonlinearly (γ = 0.5 & 0.8)	(1) Inside printer gamut: unmoved (2) Outside printer gamut: move toward the gamut shell

TABLE V. All Gamut Mapping Methods in this Experiment.

No.	Notation	Method / Coefficient Settings	Color Space
1	ID(0.5)_CAM	Image-to-Device/γ = 0.5	CIECAM97s-JCh
2	ID(0.8)_CAM	Image-to-Device/γ = 0.8	CIECAM97s-JCh
3	ID(1.0)_CAM	Image-to-Device/γ = 1.0	CIECAM97s-JCh
4	DD(0.5)_CAM	Device-to-Device/γ = 0.5	CIECAM97s-JCh
5	DD(0.8)_CAM	Device-to-Device/γ = 0.8	CIECAM97s-JCh
6	DD(1.0)_CAM	Device-to-Device/γ = 1.0	CIECAM97s-JCh
7	Clip_CAM	Clipping	CIECAM97s-JCh
8	ID(0.5)_Lab	Image-to-Device/γ = 0.5	CIEL*a*b*
9	ID(0.8)_Lab	Image-to-Device/γ = 0.8	CIEL*a*b*
10	ID(1.0)_Lab	Image-to-Device/γ = 1.0	CIEL*a*b*
11	DD(0.5)_Lab	Device-to-Device/γ = 0.5	CIEL*a*b*
12	DD(0.8)_Lab	Device-to-Device/γ = 0.8	CIEL*a*b*
13	DD(1.0)_Lab	Device-to-Device/γ = 1.0	CIEL*a*b*
14	Clip_Lab	Clipping	CIEL*a*b*

[Steps 1 & 2] Using Eq. 6 based on sRGB standard,[10] the sRGB data of test image are converted into the XYZ tristimulus values and then transformed into CIE L*a*b* and CIECAM97s-JCh space. According to Table I, test image colors are segmented into six main hue-leaves $\boldsymbol{K}_i$ $(i = r,y,g,c,b,m)$.

$$\begin{bmatrix} X \\ Y \\ Z \end{bmatrix} = \begin{bmatrix} 0.4124 & 0.3576 & 0.1805 \\ 0.2126 & 0.7152 & 0.0722 \\ 0.0193 & 0.1192 & 0.9505 \end{bmatrix} \cdot \begin{bmatrix} R_{sRGB} \\ B_{sRGB} \\ G_{sRGB} \end{bmatrix} \tag{8}$$

After image segmentation, the L-C distributions of the image ${}_{img}\boldsymbol{D}_i$ $(i = r,y,g,c,b,m)$ are plotted in CIEL*a*b* and CIECAM97s-JCh spaces. The gamut boundary functions of image ${}_{mor}\boldsymbol{F}_i$ $(i = r,y,g,c,b,m)$ are calculated.

[Step 3] As well, the L-C distributions of the sRGB monitor ${}_{mor}\boldsymbol{D}_i$ $(i = r,y,g,c,b,m)$ are segmented into the same hue-leaves, and the measured values on the hardcopy chips by inkjet printer are also segmented into the six main hue-leaves references to the hue-division LUTs. After getting the L–C distributions in each hue-leaf of the devices, the gamut boundary functions of monitor ${}_{mor}\boldsymbol{F}_i$ and printer $\boldsymbol{prtF}_i$ $(i = r,y,g,c,b,m)$ are calculated.

[Step 4] The L-C distributions of image ${}_{img}\boldsymbol{D}_i$ are compared with printer gamut boundary function ${}_{prt}\boldsymbol{F}_i$. If the segmented image colors fall inside of ${}_{prt}\boldsymbol{F}_i$, skip to Step 6 and if falls outside of ${}_{prt}\boldsymbol{F}_i$, go to Step 5.

[Step 5] To perform gamut mapping, GMAs in L–C planes are applied to all pixels of the test image and the gamma-compression coefficient γ are decided according to the measured gradation charts.

Because the optimum γ values for all color hues lie in the range of 0.7 ~ 0.9 in CIEL*a*b*, and 0.6 ~ 0.8 in CIECAM97s-JCh, γ = 0.8 will be regarded as an appropriate setting of gamma-compression coefficient for both CIELab and CIECAM97s-JCh spaces in our next steps.

[Steps 6, 7 & 8] In the hardcopies, color correction is indispensable to convert RGB data into CMY signals. For example, (1) Neugebauer equation in the halftone printing model, (2) color masking functions in the color density model of color photography, and (3) the color conversion LUTs, are used for color correction. In this study, the color correction LUTs embedded in ColorSync® profiles are applied to RGB to CMY conversion. The tested GMAs in the experiment are summarized in Table IV and all kinds of mapping tests in the experiment are listed in Table V. In both CIE L*a*b* and CIECAM97s-JCh spaces, D-D linear compression (D-D = 1.0)), two kinds of D-D nonlinear compression (D-D = 0.8) and D-D = 0.5)), I-D linear compression (I-D = 1.0)), two kinds of I-D nonlinear compression (I-D = 0.8) and I-D = 0.8)) and Clipping method are probed. Totally 14 hardcopies (GMAs x 2 spaces) are produced.

[Step 9] Detailed settings for gamut mapping experiments are listed in Table VI; the monitor's white

TABLE VI. Detailed Settings for Gamut Mapping Experiment

(1) Hardcopy Image
1. observation in light booth
2. illuminance white: D_{65}
3. luminance level: 80 cd/m^2
4. printed out by inkjet printer with high quality
5. color correction: ColorSync® profile (ICC format)
6. visual evaluation: a paired-comparison method

(2) Monitor Image
1. located at the center of CRT monitor
2. color temperature: 6500 K
3. luminance level: 80 cd/m^2
4. reference primaries (RGB) chromaticities: sRGB standard
5. the transformed matrix (XYZ to sRGB): sRGB standard
6. CRT gamma value: 2.2

(3) Viewing Surrounding
1. observe CRT & hardcopy images in a dim room
2. ambient illuminance level: 64 lux
3. observers: 12 students of normal color vision
4. viewing technique: a simultaneous binocular viewing technique

TABLE VII. Setting Parameters of View Surroundings for CIECAM97s.

Setting/Devices	Monitor Image	Hardcopy Image
luminance source	D65	D65
Tristimulus values of source white		
(measured values)	X_w = 95.0	X_w = 95.6
	Y_w = 100.0	Y_w = 100.0
	Z_w = 108.9	Z_w = 109.2
luminance level (cd/m2)	80.7	82.0
luminance of adapting field (cd/m2)	16.1	16.4
relative luminance of background (%)	20	20
ambient illuminance level (lux)	64	64
the constant for the impact of surround	0.59 (dim surround)	
the chromatic induction factor	1.1 (dim surround)	
the lightness contrast factor	1.0 (dim surround)	
the factor degree of adaptation	0.5 (incomplete chromatic adaptation)	

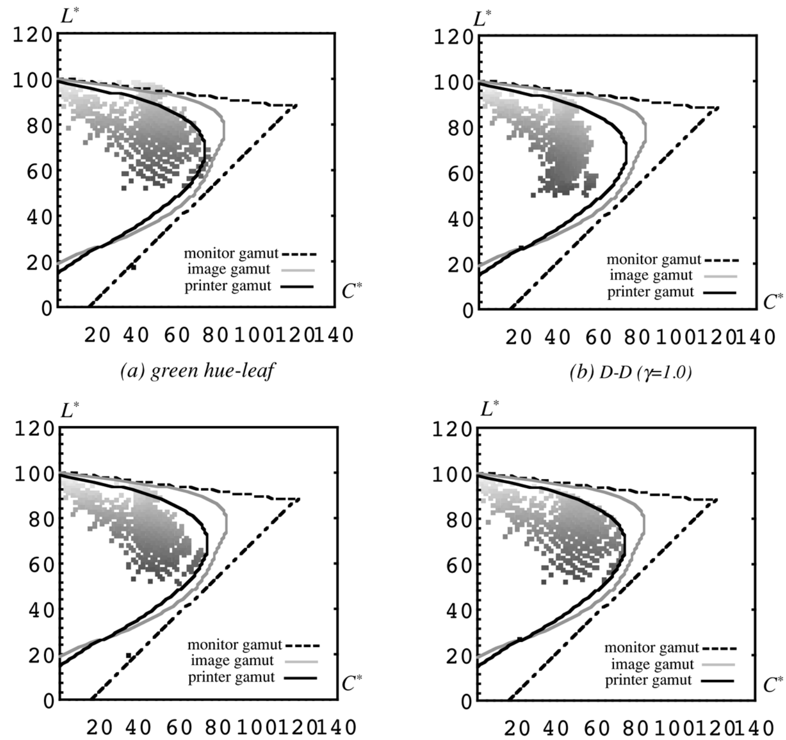

(a) green hue-leaf (b) D-D (γ=1.0) (c) I-D (γ=0.8) (d) Clipping

Figure 10. Hue-leaf of green broccoli and its L-C distributions after mapping (in CIEL*a*b* space).

point is set to the chromaticity near CIE Illuminance D_{65}. The printed hardcopies after mapping are viewed in a light booth with the same color temperature and peak luminance as the monitor. The CRT monitor is calibrated to near sRGB standard. Because the influence from color appearance factors must be considered, the tristimulus values of source white on monitor image and hardcopy image are measured with the luminance colormeter and the relational factors of CIECAM97s are set according to the practice viewing surrounding (see Table VII).

For evaluating each part of a test image, a psychophysical experiment was carried out to make a comparison of color matching between the original CRT image (right side) and the printed hardcopies after mapping (left side). A paired-comparison technique[8] is used and

TABLE VIII. The Evaluation Results of 6 Subimages T1 ~ T6: z-score Values.

GMA Subimage	T1	T2	T3	T4	T5	T6	Mean (T1 ~ T6)
ID(0.5)_CAM	0.303	0.502	0.701	0.127	0.830	0.842	0.551
ID(0.8)_CAM	0.430	1.028	0.751	0.577	0.712	0.837	0.723
ID(1.0)_CAM	0.158	0.266	0.742	–0.077	0.760	0.738	0.431
DD(0.5)_CAM	–0.669	0.010	–1.244	–1.392	0.078	0.515	–0.454
DD(0.8)_CAM	0.133	0.392	0.032	–0.227	0.140	0.705	0.196
DD(1.0)_CAM	–1.196	–0.457	–2.025	–1.616	–0.029	0.296	–0.838
Clip_CAM	0.465	0.834	0.830	–0.384	–0.427	0.839	0.360
ID(0.5)_Lab	–0.089	–0.881	0.241	–0.590	–0.107	–0.659	–0.348
ID(0.8)_Lab	0.180	0.600	0.264	0.180	0.320	1.384	0.488
ID(1.0)_Lab	–0.301	–0.710	–0.702	–0.680	0.240	–0.666	–0.470
DD(0.5)_Lab	–0.378	–1.017	–0.328	–0.620	–0.330	–0.820	–0.582
DD(0.8)_Lab	0.102	0.500	0.150	–0.058	–0.020	–0.553	0.020
DD(1.0)_Lab	–0.876	–1.637	–1.362	–1.219	0.024	–1.009	–1.013
Clip_Lab	0.967	0.730	1.256	0.332	–1.958	–0.670	0.110

(z-score values)

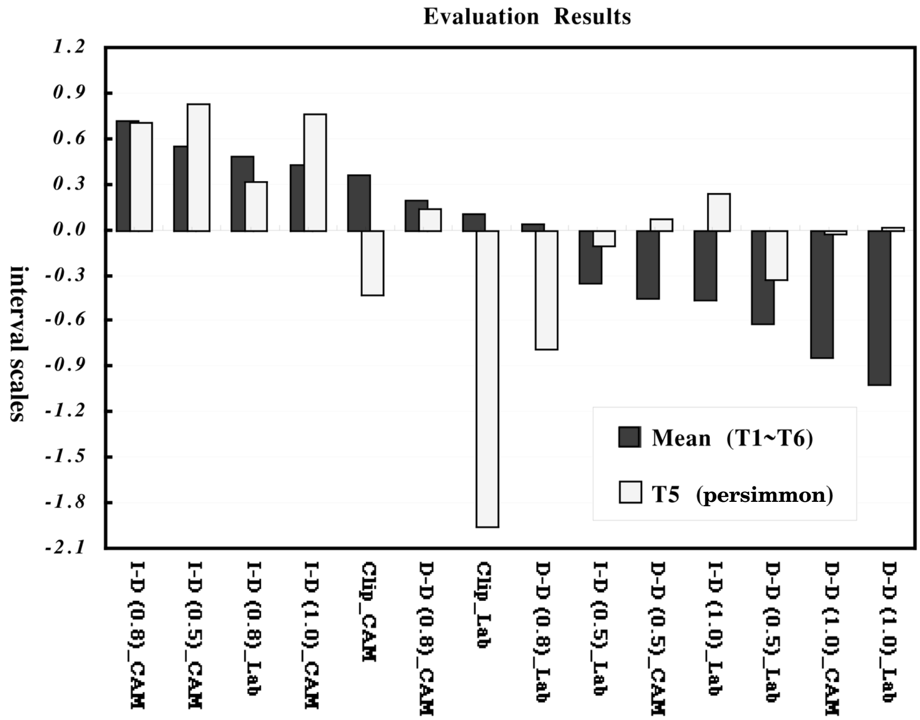

Figure 11. Evaluation results for test image. (_CAM represents CIECAM97s-JCh space and _Lab represents CIEL*a*b* space).

both images were evaluated by 12 observers in a dim viewing surroundings where the ambient illumination is approximately 64 lux. Using Thurstone's law of comparative judgement,[9] the data from the psychophysical experiment are analyzed and reproduced as interval scales (z-score).

Results

The C-L distributions after mapping are shown in Fig. 10. Clipping GMA in (d) shows that the C-L distributions are unchanged inside the printer gamut, while the gradations are lost outside the printer gamut. In contrast, D-D linear GMA in (b) keeps most of the gradations, however, the brilliant colors are compressed too much. To conquer these two faults, I-D nonlinear GMA in (c) works to keep good balance of gradation and brilliance of colors.

Table VIII shows the z-score values and Fig. 11 demonstrates the evaluation results in the psychophysical experiment. The horizontal axis shows the names of 14 kinds of mapping methods and the vertical axis means interval scale (z-score). The title of "Average (T1 ~ T6)" represents the average value of all the six component images. The title of "T5 (persimmon)" represents only the z-score values for T5: persimmon image.

The results show that proposed I-D nonlinear GMA of $\gamma = 0.8$ in CIECAM97s-JCh (i.e. *ID(0.8)_CAM*) is the best of all GMAs, and CIECAM97s (i.e., *_CAM*) space works better than CIEL * a * b * (i.e., *_Lab*) for gamut mapping. Both

TABLE IX. The Evaluation Results of 6 Subimages T1 ~ T6: Rank Orders.

GMA Subimage	T1	T2	T3	T4	T5	T6	Mean (T1 ~ T6)
ID(0.5)_CAM	4	5	5	4	1	2	2
ID(0.8)_CAM	3	1	3	1	3	4	1
ID(1.0)_CAM	6	8	4	6	2	5	4
DD(0.5)_CAM	12	9	12	13	7	7	10
DD(0.8)_CAM	7	7	9	7	6	6	6
DD(1.0)_CAM	14	10	14	14	10	8	13
Clip_CAM	2	2	2	8	13	3	5
ID(0.5)_Lab	9	12	7	9	11	10	9
ID(0.8)_Lab	5	4	6	3	4	1	3
ID(1.0)_Lab	10	11	11	11	5	11	11
DD(0.5)_Lab	11	13	10	10	12	13	12
DD(0.8)_Lab	8	6	8	5	9	9	8
DD(1.0)_Lab	13	14	13	12	8	14	14
Clip_Lab	1	3	1	2	14	12	7

(rank orders)

Figure 12. False centours in the persimmon (the boundary between red and yellow colors) of CG image and improvement by I-D Gamma-Compression.

I-D GMAs with $\gamma = 0.8$ (i.e., *ID(0.8)_CAM* and *ID(0.8)_Lab*) have higher z-score values than other GMAs.

Because Clipping GMA maps the highlight colors to the outer shell of printer gamut, heavy false contours appear for the persimmon image (see Fig. 12). This is the reason why the persimmon image has lower z-score values for Clipping GMA (*Clip_CAM* and *Clip_Lab*) than other subimages. When the same g values are set, all I-D GMAs have better results than D-D compressions in two color spaces (e.g., ID(0.5)_CAM is better than DD90.5)_CAM, etc., see Table IX.

Conclusions

Image-to-Device GMAs coupled with the hue-leaf division and image gradation scaling are proposed. The optimum range of the gamma compression coefficient γ lies around 0.8 in CIE L*a*b* and CIECAM97s-JCh space. The evaluation results show that I-D nonlinear compressions are better than D-D linear compressions in both color spaces. In the experiments, a single image including six partial images with variety of rendition characteristics, CIECAM97s-JCh space worked better than CIEL*a*b* for gamut compression. However, the calculations in CIECAM97s-JCh space require much more computational cost than CIEL*a*b*. A simpler and higher speed GMA in CIECAM97s-JCh is excepted to be developed.

References

1. G. J. Braun and M. D. Fairchild, Gamut mapping for Pictorial Images, *Proc. TAGA*, 645–660 (1999).
2. M. D. Fairchild, *Color Appearance Models*, Addison-Wesley, pp. 384–389 (1998).
3. N. Katoh, Masahiko Ito and S. Ohno, Three-dimensional Gamut mapping using various color difference formulae and color spaces, *J. Electron. Imaging* **8,** 365–379 (1999).
4. C.-S. Lee, C.-H. Lee and Y.-H. Ha, Parametic Gamut mapping Algorithms using variable anchor points, *J. Imaging Sci. Technol.* **44,** 1, 68–73 (2000).
5. J. Morovic and M. Ronnier Luo, Gamut mapping algorithms based on psychophysical experiment, *Proc. 5th IS&T/SID CIC*, IS&T, Springfield, VA, 1997, pp. 44–49.
6. C. Hung-Shing, M. Omamiuda and H. Kotera, Adaptive Gamut Mapping Method Based on Image-to-Device, *Proc. IS&T NIP15*, IS&T, Springfield, VA, 1999, pp. 346–349.
7. K. M. Braun, M. D. Fairchild and P. J. Alessi, Viewing Techniques for Cross-Media Image Comparisons, *Color Res. Appl.* **21,** 6–17 (1996).
8. L. L.Thurstone, A Law of Comparison Judgement, *Psych. Review*, 273-289 (1927).
9. T.-C. Hseue, Y.-C. Shen, P.-C. Chen, W.-H. Hue, and Y.-T. Liu, Cross-Media Performance Evaluation of Color Medels for Unequal Luminance Levels and Dim Surround, *Color Res. Appl.* **23,** 169–177 (1998).
10. A Standard Default Color Space for the Internet-sRGB, http://www.w3.org/Graphics/Color/sRGB